

# KEWS: A KPIs-Based Evaluation Framework of Workload Simulation On Microservice System

Pengsheng Li, Qingfeng Du\*, and Shengjie Zhao  
School of Software Engineering, Tongji University  
Shanghai, China  
{2131514, du\_cloud, shengjiezhao}@tongji.edu.cn

**Abstract**—Simulating the workload is an essential procedure in microservice systems as it helps augment realistic workloads whilst safeguarding user privacy. The efficacy of such simulation depends on its dynamic assessment. The straightforward and most efficient approach to this is comparing the original workload with the simulated one using Key Performance Indicators (KPIs), which capture the state of the system. Nonetheless, due to the extensive volume and complexity of KPIs, fully evaluating them is not feasible, and measuring their similarity poses a significant challenge. This paper introduces a similarity metric algorithm for KPIs, the Extended Shape-Based Distance (ESBD), which gauges similarity in both shape and intensity. Additionally, we propose a KPI-based Evaluation Framework for Workload Simulations (KEWS), comprising three modules: preprocessing, compression, and evaluation. These methodologies effectively counteract the adverse effects of KPIs’ characteristics and offer a holistic evaluation. Experimental results substantiate the effectiveness of both ESBD and KEWS.

**Index Terms**—workload simulation, key performance indicators, microservice system, similarity metric

## I. INTRODUCTION

Workload simulation serves as a vital task to augment the realistic workload, the fundamental data source for AI operations (AIOps) in microservice systems [1]. Such workloads are crucial for various applications such as anomaly detection and root cause analysis [2]. This task involves the extraction and processing of features from the realistic workload, enabling the generation of a simulated workload bearing similar properties. Evaluating workload simulations necessitates not just static comparisons of workload characteristics [3], but also dynamic assessments of system status under both realistic and simulated workloads. Key Performance Indicators (KPIs), which record the internal status of systems in a structured time-series format [4], are indisputably the most typical monitoring data within microservice systems [5]. Nevertheless, three significant challenges confront the evaluation of workload simulations using KPIs in microservice systems.

Firstly, monitoring an enormous quantity of KPIs within microservice systems for real-time anomaly detection renders their use impractical for evaluation purposes. Secondly, the characteristics of KPIs are more complex relative to ideal time series, entailing various elements including amplitude differences, phase shifts, inevitable noise, high dimensionality, and large numerical spans. These characteristics alter the shape

and intensity of the KPIs, thereby warping the similarities. Thirdly, the intricate characteristics of KPIs result in a shortage of suitable similarity metrics applicable to them.

To address these issues, we introduce an extended shape-based distance (ESBD) algorithm as a similarity metric for KPIs, taking into account both shape and intensity. Moreover, we examine a novel framework for workload simulation evaluation, which is the KPIs-based Evaluation Framework of Workload Simulation (KEWS). Our approach begins with preprocessing KPIs to diminish their complex characteristics. Subsequently, we generate representative sets of KPIs using a Domain Knowledge Filter (DKF), a Chaos Experiment Filter (CEF), and a Dynamic Time Warping (DTW)-based Density Adaptive DBSCAN Cluster. Finally, with these KPI sets, we assess the quality of the workload simulation employing ESBD. Our contributions can be summarized as follows:

- We introduce a novel similarity metric algorithm for KPIs, ESBD, which discerns similarity by evaluating both shape and intensity.
- We propose a new, more practical framework for assessing workload simulation than currently existing models. To the best of our knowledge, this stands as the first attempt to evaluate workload simulation using KPIs.
- We conduct comprehensive experiments to corroborate the effectiveness of both ESBD and KEWS by comparing these with baseline methods.

## II. RELATED WORK

### A. KPI Similarity Metric

The KPI similarity metric is widely used as both an absolute criterion for making statistical inferences regarding KPI inter-relationships and a relative measure for downstream tasks [6], [7], which can be categorized primarily into two types: raw-based and feature-based methods. Raw-based methods directly calculate the similarity of KPIs, drawing on approaches such as Shape-based Distance (SBD) [8] and Dynamic Time Warping (DTW) [9], [10]. Alternatively, feature-based methods map KPIs into low-dimensional latent spaces to learn representations for similarity, deploying techniques like the transformer-based method [11] and contrastive learning method [12]. Even though raw-based methods are better suited for precise workload evaluation, a majority of current techniques focus only on shape similarity while neglecting intensity.

\*Corresponding author: Qingfeng Du

## B. Workload Simulation Evaluation

Being among the minority of studies addressing workload simulation evaluation, WESSBAS [3] evaluates workload using static statistics, thereby overlooking dynamic features. A crucial aspect of evaluating workload simulation dynamically lies in the discerning selection of suitable KPIs from a vast pool [13]. Given the explicit or subtle correlations between KPIs [4], one can extract homogeneous KPIs through clustering. In recent times, there's been a fresh line of research investigating clustering algorithms for KPIs, such as the K-shape based method [14], hierarchical-based method [15], and density-based methods [16]–[18]. However, these methods focus solely on the value characteristics and disregard the intrinsic attribute characteristics of the KPI, which results in an information loss.

### III. PROBLEM DEFINITION

In this section, we present a set of formal descriptions for quality evaluation of workload simulation.

**Definition 1 (Workload Simulation):** Given a workload  $\mathcal{W}$  of a microservice system  $\mathcal{M}$ , workload simulation aims to generate a new workload  $\mathcal{W}'$  of  $\mathcal{M}$  with properties of  $\mathcal{W}$ .

**Definition 2 (Workload Evaluation):** Given data  $\mathcal{D}, \mathcal{D}'$  obtained by injecting original  $\mathcal{W}$  and simulated workload  $\mathcal{W}'$  into the system  $\mathcal{M}$ , the target of workload evaluation  $h(\mathcal{D}, \mathcal{D}')$  is to measure the workload similarity between  $\mathcal{W}$  and  $\mathcal{W}'$ .

**Definition 3 (Similarity Metric):** Given two time series  $\mathbf{x} \in \mathbb{R}^{m_x}, \mathbf{y} \in \mathbb{R}^{m_y}$ , the target of similarity metric  $\phi(\mathbf{x}, \mathbf{y})$  is to calculate the similarity  $\Phi$  sparing the shape variations, e.g., noise, amplitude differences and phase shifts.

### IV. METHODOLOGY

As illustrated in Fig.1, KEWS comprises three components: pre-processing, compression, and evaluation. Initially, the corresponding KPIs are produced by injecting both the original workload  $\mathcal{W}$  and the simulated workload  $\mathcal{W}'$  into the system. Following this, the KPIs are refined into increment-centric, low-noise, standardized data during the pre-processing stage. Subsequently, the compression of KPIs leverages original workload KPIs to condense the KPIs evaluation set. This process utilizes domain knowledge and chaos experiments in conjunction with ESBD for strong correlation and employs a DTW-based Density Adaptive DBSCAN clustering model for weak correlation. Finally, in the KPIs evaluation phase, ESBD is utilized to evaluate the similarity between the original and the simulated workload. The results are then aggregated to characterize the overall quality of the workload simulation.

#### A. Similarity Metric

We propose the Extended-Shape-Based Distance (ESBD) as a comprehensive similarity metric for KPIs across varying scales. This consistent metric concurrently measures similarity in both shape and intensity. For ease of understanding, we exemplify ESBD using scenarios where the lengths of the KPIs are identical. It is crucial to note that ESBD is equally

applicable in situations where these lengths differ. Formally, let  $\mathbf{x}_1, \mathbf{x}_2 \in \mathbb{R}^m$  denote two KPI time series of length  $m$ , as:

$$\phi_{esbd}(\mathbf{x}_1, \mathbf{x}_2) := (1-\alpha)\phi_{shape}(\mathbf{x}_1, \mathbf{x}_2) + 2\alpha\phi_{intensity}(\mathbf{x}_1, \mathbf{x}_2), \quad (1)$$

where  $\phi_{shape}(\cdot)$  measures the shape similarity of the KPIs, while  $\phi_{intensity}(\cdot)$  gauges their intensity similarity. We assign  $\alpha \in [0, 1]$  as the intensity factor, which controls the balance between shape and intensity. Importantly,  $\phi_{shape}(\cdot)$  employs the cross-correlation-based SBD method [8] to depict KPI shape similarity, which can be formulated as:

$$\phi_{shape}(\mathbf{x}_1, \mathbf{x}_2) := 1 - \max_l \left( \frac{R_{l-m}(\mathbf{x}_1, \mathbf{x}_2)}{\sqrt{R_0(\mathbf{x}_1, \mathbf{x}_1) \cdot R_0(\mathbf{x}_2, \mathbf{x}_2)}} \right), \quad (2)$$

where  $l \in \{1, 2, \dots, 2m-1\}$  is the series phase shift index.  $R_k(\cdot)$  is the cross-correlation function, as shown in (3):

$$R_k(\mathbf{x}_1, \mathbf{x}_2) := \begin{cases} \sum_{l=1}^{m-k} x_{1,l+k} \cdot x_{2,l}, & k \geq 0 \\ R_{-k}(\mathbf{x}_2, \mathbf{x}_1), & k < 0 \end{cases}, \quad (3)$$

where  $k$  is the relative phase shift index between  $\mathbf{x}_1, \mathbf{x}_2$ . From the cross-correlation property,  $\phi_{shape} \in [0, 2]$ , and the smaller  $\phi_{shape}$  indicates a higher shape similarity between  $\mathbf{x}_1$  and  $\mathbf{x}_2$ .

We posit that the similarity of the KPIs' intensity is predominantly reflected through the similarity of their peak intensity. As such,  $\phi_{intensity}(\cdot)$  computes the ratio of the peak mean values between  $\mathbf{x}_1, \mathbf{x}_2$ , which can be expressed as follows:

$$\phi_{intensity}(\mathbf{x}_1, \mathbf{x}_2) := \exp\left\{ \frac{-1}{|q(\mathbf{x}_1, \mathbf{x}_2) - 1|} \right\}, \quad (4)$$

where  $q(\mathbf{x}_1, \mathbf{x}_2)$  is the peak ratio function, described by the similarity between peaks of  $\mathbf{x}_1$  and  $\mathbf{x}_2$ , as shown in:

$$q(\mathbf{x}_1, \mathbf{x}_2) := \max\left( \frac{\frac{1}{n_1} \sum v_{x_1}^i}{\frac{1}{n_2} \sum v_{x_2}^i}, \frac{\frac{1}{n_1} \sum v_{x_2}^i}{\frac{1}{n_2} \sum v_{x_1}^i} \right), \quad (5)$$

where  $v_{x_1}^i, v_{x_2}^i$  are the peaks value of  $\mathbf{x}_1, \mathbf{x}_2$ , and  $n_x, n_y$  are the peak number of  $\mathbf{x}_1, \mathbf{x}_2$  respectively. In this context, a smaller  $\phi_{intensity}$  indicates a higher similarity between  $\mathbf{x}_1, \mathbf{x}_2$  in terms of intensity. Additionally,  $\phi_{intensity}$  is more sensitized when  $\mathbf{x}_1, \mathbf{x}_2$  exhibit similar intensity levels. Here,  $q$  functions as a temperature parameter.

In summary,  $\phi_{esbd}$  lies within the range of  $[0, 2]$ . Lower values of  $\phi_{esbd}$  suggest higher similarity between KPIs, modulated by the intensity factor  $\alpha$ . Generally, we set the intensity factor  $\alpha$  to 0.5 and use 1.0 as the ESBD similarity threshold.

#### B. pre-processing

The pre-processing  $p(\cdot)$  aims to transform the raw workload KPIs  $\tilde{\mathbf{X}}$  into incremental, low-noise, standardized KPIs  $\mathbf{X}$ . Toward this end, we sequentially apply five pre-processing steps: imputation  $p_{im}(\cdot)$ , differentiation  $p_{diff}(\cdot)$ , resampling  $p_{rs}(\cdot)$ , denoising  $p_{dn}(\cdot)$  and standardisation  $p_{std}(\cdot)$ . It's important to note here that the KPIs that are utilized for the final evaluation do not undergo the standardization step  $p_{std}(\cdot)$ .

**Imputation.** Given the typically low probability of KPI values missing, a straightforward and efficient method is used to address this issue. Specifically, cubic spline interpolation is applied to segments with missing values, as follows:

$$\tilde{\mathbf{X}}_{i,j:k}^{(im)} = p_{im}(\tilde{\mathbf{X}}_{i,j:k}, l) := \text{CubicSpline}(\tilde{\mathbf{X}}_{i,j-l:k+l}), \quad (6)$$

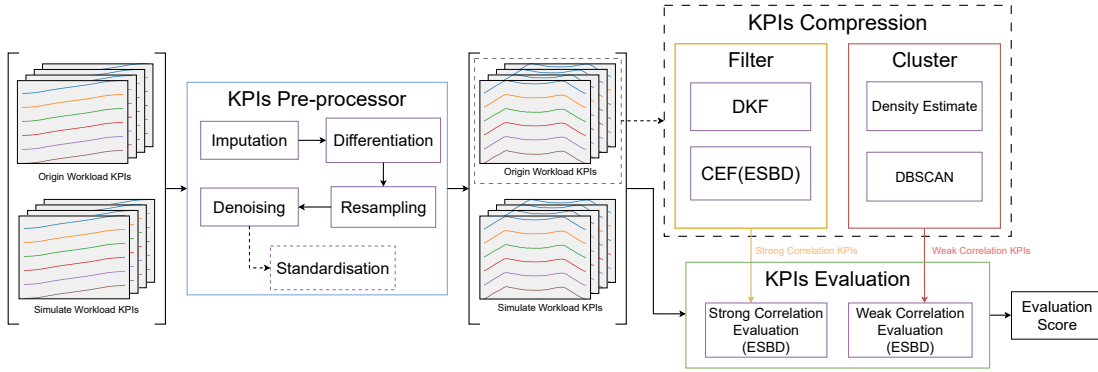


Fig. 1: The overall pipeline of KEWS.

where  $\tilde{\mathbf{X}}_{i,j:k}$  is  $\tilde{\mathbf{X}}_i$  with the missing value segment ( $j : k$ ), and the non-missing values at segment ( $j - l : k + l$ ) are the interpolation point, while  $l$  is the interpolation interval length. **Differentiation.** In order to effectively highlight the incremental features that emphasize real-time characteristics, we apply the first-order differential to cumulative KPIs, as follows:

$$\tilde{\mathbf{X}}_i^{(diff)} = p_{diff}(\tilde{\mathbf{X}}_i^{(im)}) := \tilde{\mathbf{X}}_{i,1:m-1}^{(im)} - \tilde{\mathbf{X}}_{i,0:m-2}^{(im)}. \quad (7)$$

**Resampling.** For an analysis aligning with certain levels of granularity, specific periods—such as macroscopic time intervals—should be used for macroscopic periods. To synchronize these time intervals with the corresponding periods, resampling is performed on KPIs. Suppose  $\tau$  signifies a suitable time interval and  $\Delta t$  is the default time interval of the KPI. Now, the resampling process would proceed as follows:

$$\tilde{\mathbf{X}}_i^{(rs)} = p_{rs}(\tilde{\mathbf{X}}_i^{(diff)}) := \left\| \sum_{j=0}^{m'} \tilde{\mathbf{X}}_{i,j+k}^{(diff)}, \quad (8)$$

where  $l = \lfloor \frac{\tau}{\Delta t} \rfloor$  is the ratio of resample, and  $m' = \lfloor \frac{m}{l} \rfloor$  is the length of KPIs after resample operation while  $\tilde{\mathbf{X}}_i^{(rs)} \in \mathbb{R}^{n \times m'}$ .

**Denoising.** To address the random noise inherent in the KPIs, we will apply the Kalman filter [19] to the KPIs  $\tilde{\mathbf{X}}_i^{(rs)}$ :

$$\tilde{\mathbf{X}}_i^{(dn)} = p_{de}(\tilde{\mathbf{X}}_i^{(rs)}) := \text{KalmanFilter}(\tilde{\mathbf{X}}_i^{(rs)}). \quad (9)$$

**Standardisation.** There exist potential relationships between KPIs at differing scales and KPI compression only considers similarities in shape, not differing magnitudes. Therefore, to align and compare these KPIs, standardisation is applied as:

$$\mathbf{X}_i = p_{std}(\tilde{\mathbf{X}}_i^{(dn)}) := \frac{\tilde{\mathbf{X}}_i^{(dn)} - \mu_i}{\sigma_i}, \quad (10)$$

where  $\mu_i$  is the mean of  $\tilde{\mathbf{X}}_i^{(dn)}$  and  $\sigma_i$  is the standard deviation.

### C. Compression

Microservice systems typically host an extensive array of KPIs, which can complicate individual analyses for evaluation purposes. Moreover, different workload simulation tasks usually contain varied business logic, enhancing the representativeness of business-related KPIs for these workload patterns. However, this does not imply the irrelevance of business-independent KPIs. To address this, we design a KPI filter and a KPI cluster mechanism to categorize all KPIs  $\mathcal{K}$  into strongly correlated KPIs  $\mathcal{K}_s$  and weakly correlated KPIs  $\mathcal{K}_w$ , based

on their relevance to business operations. Specifically, the KPI filter leverages domain knowledge and chaos experiments [20] to derive  $\mathcal{K}_s$ , while the KPI clustering mechanism selects a subset of representative weakly correlated KPIs  $\mathcal{K}_w$  from  $\mathcal{K}$ .

1) **Filter:** The KPIs filter is bifurcated into coarse filter by domain knowledge and refined filter by chaos experiments. **Domain Knowledge Filter.** In microservice systems, KPIs are typically distinguished by fine-grained label attributes and coarse-grained domain attributes. The former encapsulates specific characteristics, while the latter reflects categorical traits, such as application source (like ENVOY or ISTIO), and monitoring level (like NODE or NETWORK). Accordingly, through the lens of domain attributes, we can examine the relevance of KPIs to the business, thereby establishing a coarse-grained filter, denoted as DKF. This filter yields the coarse-grained KPI set  $\mathcal{K}_c$ .

**Chaos Experiments Filter.** We deploy chaos experiments to extract the fine-grained KPI set  $\mathcal{K}_s$  from  $\mathcal{K}_c$ . This is part of a refined filtering process, denoted as CEF, which injects the same workload under varying perturbations. We model these correlations by calculating the steady-state deviations of KPIs relative to business-independent faults. The divergence between these steady-states informs us about the relevance of KPIs, aiding in their fine-graining.

Our chaos experiment is organized into two control and one experimental group. The control groups provide a steady-state baseline for the system, maintained without the introduction of any perturbations. In contrast, the experimental group is subjected to a set of business-independent perturbations, denoted  $\delta$ . For a specific KPI  $k$ , instances  $\mathbf{x}_1$  and  $\mathbf{x}_2$  stand for the control group's KPI measurements, while  $\tilde{\mathbf{x}}$  denotes the one from the experimental group. The interrelation among  $\mathbf{x}_1, \mathbf{x}_2, \tilde{\mathbf{x}}$  can be mathematically formulated as follows:

$$\begin{aligned} \mathbf{x}_2 &= \mathbf{x}_1 + \boldsymbol{\varepsilon}, \\ \tilde{\mathbf{x}} &= \mathbf{x}_1 + \lambda \boldsymbol{\delta} + \tilde{\boldsymbol{\varepsilon}}, \\ \boldsymbol{\varepsilon} &\neq \tilde{\boldsymbol{\varepsilon}}, \end{aligned} \quad (11)$$

where  $\lambda \in [0, 1]$  is the degree of the  $\delta$  perturbations,  $\boldsymbol{\varepsilon}, \tilde{\boldsymbol{\varepsilon}}$  are the inherent system errors. The term  $\lambda \boldsymbol{\delta}$  denotes the steady-state offset in response to perturbations; a larger value of  $\lambda$  implies that  $k$  is more susceptible to the perturbations  $\boldsymbol{\delta}$  and holds a lesser relevance to the business operations.

Despite this, precise calculations of  $\lambda$  and  $\delta$  or deriving the exact value of  $\lambda\delta$ , are challenging tasks. We therefore estimate  $\lambda\delta$  by quantifying the relevance to business operations through the contrastive analysis of ESB D among  $\mathbf{x}_1, \mathbf{x}_2, \tilde{\mathbf{x}}$ . Let  $\phi_{esbd}(\mathbf{x}_1, \mathbf{x}_2), \phi_{esbd}(\mathbf{x}_1, \tilde{\mathbf{x}}), \phi_{esbd}(\mathbf{x}_2, \tilde{\mathbf{x}})$  symbolize intra-group and inter-group ESB D respectively, denoted for simplicity as  $\Phi_0, \Phi_1, \Phi_2$ . We introduce a perturbation coefficient as a measure of the KPI's perturbability, expressed as:

$$r(\Phi_0, \Phi_1, \Phi_2) := \max(\log \frac{\exp^{\Phi_1+\Phi_2}}{\exp^{2\Phi_0}}, \log \frac{\exp^{2\Phi_0}}{\exp^{\Phi_1+\Phi_2}}). \quad (12)$$

When the perturbation coefficient  $r$  is less than a specific threshold  $\gamma \in (0, +\infty)$ ,  $k$  is considered a strong correlation KPI. We set  $\gamma = 1$  for the following experiments.

Iterate all the  $k \in \mathcal{K}_c$ , and individually verify their compliance with the aforementioned conditions. This process identifies the set of strongly correlated KPIs  $\mathcal{K}_s$  and concurrently, determines the set of weakly correlated KPIs  $\tilde{\mathcal{K}}_w$ , which is the complement of  $\mathcal{K}_s$  in  $\mathcal{K}$ .

2) *Cluster*: To explore potential connections within KPIs, we perform clustering on the business-independent KPIs based on their shape, taking the centroid KPI in each cluster to form the weak correlation KPIs set  $\mathcal{K}_w$ .

---

#### Algorithm 1 Heuristic Density Estimation

---

**Input:**  $k_{dis}$ : DTW-based KNN curve;  
 $max\_radius$ : upper bound of the density radius;  
 $left$ : smallest index satisfies  $k\_dist[left] \leq max\_radius$ ;  
 $right$ : largest index;  
 $len\_thresh$ : threshold of segment length;  
 $slope\_thresh$ : threshold of slope;  
 $slope\_diff\_thresh$ : threshold of difference between slopes;  
**Output:**  $radius\_index$ : index of largest candidate radius.

```

1: function RADIUS_ESTIMATION( $k_{dis}, left, right$ )
2:   if  $right - left < len\_thresh$  then
3:     return // Search area is too small;
4:   end if
5:   if  $left < 0$  or  $right < 0$  then
6:     return // No flat portion from the last step
7:   end if
8:    $index \leftarrow -1, radius\_index \leftarrow -1, diff \leftarrow max\_radius$ ;
9:   for  $i = (left + 1) \rightarrow i = right$  do
10:     $left\_slope \leftarrow -(k_{dis}[i] - k_{dis}[left]) / (i - left)$ ;
11:     $right\_slope \leftarrow -(k_{dis}[i] - k_{dis}[right]) / (i - right)$ ;
12:    if  $left\_slope > slope\_thresh$  and  $right\_slope > slope\_thresh$  then
13:      continue; // Prune the steep portion
14:    end if
15:    if  $|left\_slope - right\_slope| < diff$  then
16:       $diff \leftarrow |left\_slope - right\_slope|, index \leftarrow i$ ;
17:    end if
18:  end for
19:  if  $diff < slope\_diff\_thresh$  then
20:     $radius\_index \leftarrow index$ 
21:  end if
22:  // Divide and Conquer
23:   $radius\_index \leftarrow \min(radius\_index, RADIUS\_ESTIMATION(k_{dis}, index, right))$ ;
24:  for  $i = (index) \rightarrow i = left$  do
25:    if  $k_{dis}[i] - k_{dis}[index] > diff$  then
26:       $index \leftarrow i$ ;
27:    break; // Search forward for the next flat portion.
28:  end if
29:   $radius\_index \leftarrow \min(radius\_index, RADIUS\_ESTIMATION(k_{dis}, left, index))$ ;
30:  return  $radius\_index$ 
31: end function

```

---

Inspired by the prior KPI clustering algorithm [16]–[18], we design a heuristic approach for density estimation to a DTW-based DBSCAN clustering model, providing adaptive density radius, as shown in Algorithm 1. The crux of our

heuristic density estimation is the identification of feasible density radius candidates on flat portions of the K-Nearest-Neighbor (KNN) curve, which represents the descending order DTW distance between each KPI instance and its K-Nearest-Neighbor, denoted as  $k_{dis}$ . Specifically, for any given point on the curve, we determine its flat portion status – indicative of a potential radius – by comparing slope differences at the left and right endpoints. We utilise a divide-and-conquer strategy to iterate over both sides of the point, identifying all potential candidates and selecting the largest as the estimated radius. This process is optimised through pruning for recursion reduction. Additionally, we adopt the upper boundary pruning methodology [21], alongside the search constraints recommended [22], to expedite DTW computation. We further enhance DBSCAN clustering efficiency by chunking KPIs within their domain attributes.

Upon obtaining a series of clusters through the DTW-based DBSCAN, we compute the centroid of each cluster as a representative KPI for evaluation, expressed as follows:

$$z_i = \arg \min_{x \in C_i} \sum_{y \in C_i} DTW(x, y), \quad (13)$$

where  $C_i$  is one of the clusters from DBSCAN, then, the KPIs  $k_i \in \tilde{\mathcal{K}}_w$  represented by the centroid of each cluster form a reduced weak correlation KPI set  $\mathcal{K}_w$ .

#### D. Evaluation

Leveraging the strong and weak correlation KPI sets  $\mathcal{K}_s$  and  $\mathcal{K}_w$ , which we obtain from above steps respectively, we apply ESB D to calculate the similarity between the original and simulated workload by aggregation with the statistical importance weights for evaluation.

**Weak Correlation Evaluation.** Given the  $i^{\text{th}}$  KPI in  $\mathcal{K}_w$ , whose instances under original and simulated workload are  $\mathbf{x}_{\mathcal{K}_w^{(i)}}, \mathbf{x}'_{\mathcal{K}_w^{(i)}}$ , we calculate the ESB D between the two, i.e.,  $\phi_{esbd}(\mathbf{x}_{\mathcal{K}_w^{(i)}}, \mathbf{x}'_{\mathcal{K}_w^{(i)}})$ , denoted as  $\Phi_{\mathcal{K}_w^{(i)}}$ , and then aggregated as:

$$\Phi_{\mathcal{K}_w} := \frac{1}{|\mathcal{K}_w|} \sum_{i=0}^{|\mathcal{K}_w|-1} \Phi_{\mathcal{K}_w^{(i)}}, \quad (14)$$

in which the arithmetic mean of  $\Phi_w$  characterises the distance between the original and the simulated workload, then normalized as a weak correlation evaluation score:

$$E_{\mathcal{K}_w} = \frac{\mu_{\mathcal{K}_w}}{\mu_{\mathcal{K}_w} + \Phi_{\mathcal{K}_w}}, \quad (15)$$

where  $\mu_{\mathcal{K}_w} \in (0, 2)$  is the similarity threshold of the weak correlation evaluation.

**Strong Correlation Evaluation.** As strong correlation KPIs monitor the state of each individual service, variances in these metrics mirror differences in workload patterns. To evaluate these KPIs, which form the foundation for workload simulation evaluation, we need a finer-grained aggregation process. Workloads generally include calls to a multiplicity of specific services. Thus, based on the types of services, we partition  $\mathcal{K}_s$  into several services subsets corresponding to individual services, denoted by  $\mathcal{K}_s^{(i)}$ , such that  $\bigcup_{i=1}^{n_t} \mathcal{K}_s^{(i)} = \mathcal{K}_s$ , where  $n_t$  is the number of service type. We also employ

the frequency of service calls as the importance weight  $\omega_i$ , satisfying  $\sum_{i=1}^{n_t} \omega_i = 1.0$ . Given the strong correlation KPIs  $k_j \in \mathcal{K}_s$ , we aggregate the ESB for evaluation as follows:

$$\Phi_{\mathcal{K}_s} := \sum_{i=1}^{n_t} \omega_i \left( \frac{1}{n_t^{(i)}} \sum_{j=1}^{n_t^{(i)}} \Phi_j \right), n_t^{(i)} = |\mathcal{K}_s^{(i)}|. \quad (16)$$

Then, normalized as follows:

$$E_{\mathcal{K}_s} = \frac{\mu_{\mathcal{K}_s}}{\mu_{\mathcal{K}_s} + \Phi_{\mathcal{K}_s}}, \quad (17)$$

in which  $\mu_{\mathcal{K}_s}$  is the similarity threshold of the strong correlation evaluation. In general, we set  $\mu_{\mathcal{K}_w} = \mu_{\mathcal{K}_s}$ .

Finally,  $E_{\mathcal{K}_w}$  and  $E_{\mathcal{K}_s}$  were weighted by the correlation factor  $\beta \in [0, 1]$  to obtain a single similarity evaluation  $E$  of the quality of the workload simulation, expressed as:

$$E = h_{\beta}(\mathcal{K}_w, \mathcal{K}_s) := (1 - \beta)E_{\mathcal{K}_w} + \beta E_{\mathcal{K}_s}. \quad (18)$$

## V. EXPERIMENTS

In this section, we conduct empirical experiments to demonstrate the effectiveness of ESB and KEWS. We aim to address the following three research questions: **RQ1**: How effective is ESB for describing similarities in shape and strength? **RQ2**: How effective is KEWS for compressing KPIs with filter and cluster? **RQ3**: How accurate is KEWS for evaluating the quality of workload simulation?

### A. Experimental Setup

**Benchmark System.** Our experiments are conducted in an open-source microservices application, *Hipstershop*<sup>1</sup>, which is a typical online e-commerce application widely used in the research of microservice operations.

**Workload Simulation.** We use *K6* to generate real-world workloads on *Hipstershop* as the original workload  $\mathcal{W}$ . As shown in Fig. 2, we set up a total of nine workload scenarios with three shapes ( $\mathcal{S}_a, \mathcal{S}_b, \mathcal{S}_c$ ) and three intensities ( $\mathcal{I}_1, \mathcal{I}_2, \mathcal{I}_3$ ). We employ LWS [23] to generate the simulated workload  $\mathcal{W}'$  and capture original log data for LWS by *Elasticsearch*<sup>2</sup> and *Filebeat*<sup>3</sup>, then capture KPIs data by *Prometheus*<sup>4</sup>.

**Baselines.** For similarity metric, we compare ESB with DTW [9] and SBD [8]. For workload simulation evaluation, we compare KEWS with WESSBAS [3].

### B. Effectiveness of ESB (RQ1)

Since the open-source KPIs dataset makes it difficult to meet the demand for shape and intensity control, we utilize the KPIs generation algorithm TSAGEN [24] to conduct the validation experiments to compare the trend between SBD and DTW. Fig. 3 reports the trend of our method ESB and other baselines with shape change and intensity change, where  $\theta_1, \theta_2$  are the shape factors and  $\theta_3$  is the intensity factor and the horizontal axis is the multiplier of the factors.

<sup>1</sup><https://github.com/GoogleCloudPlatform/microservices-demo>

<sup>2</sup><https://www.elastic.co/cn/elasticsearch/>

<sup>3</sup><https://www.elastic.co/cn/beats/filebeat>

<sup>4</sup><https://prometheus.io/docs/introduction/overview/>

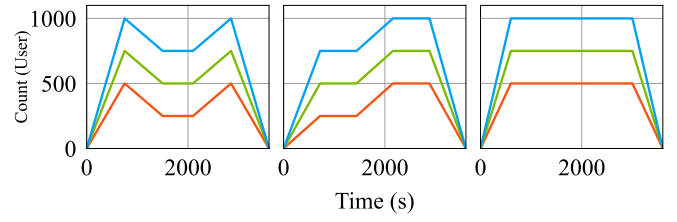


Fig. 2: Workload curve setting

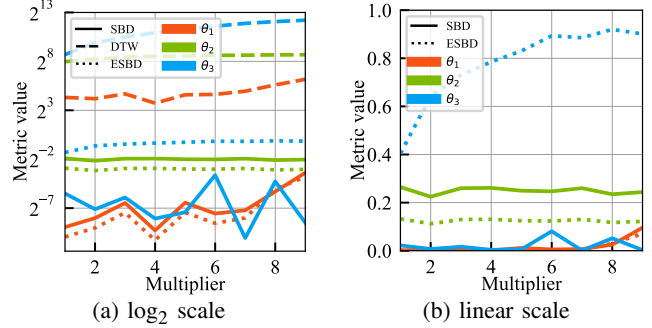


Fig. 3: Trend of metric with change of  $\theta_1, \theta_2, \theta_3$

As can be observed, the three similarity metrics have similar trends in the  $\log_2$  scale, as they can both capture shape features, while DTW has much larger values. In linear scale, Fig. 3b shows ESB's ability to capture intensity features and the same to SBD in terms of shape, which validates the effectiveness of ESB, compared to DTW and SBD.

### C. Effectiveness of Compression (RQ2)

TABLE I: Strong correlation domain attributes of KPIs

Domain	Description
container	Kubernetes Resources
grpc	Kubernetes application, monitoring grpc service
http	Kubernetes application, monitoring http requests
istio	Kubernetes component, for workload management
node	Kubernetes Resources

Based on the principle of locality and the domain knowledge of *Kubernetes*, we summarise the strong correlation KPIs as shown in Table. I, including *Kubernetes* resources and application. Then, We employ an open-source tool *ChaosMesh* to conduct our chaos experiment. As shown in Table. II, **grpc** and **istio** are the strong correlation domain KPIs described by  $\gamma = 0.1$  and  $r$ , which are much smaller than others.

TABLE II: The perturbation coefficient  $r$  of chaos experiment

Domain	$\mathcal{I}_1$			$\mathcal{I}_2$			$\mathcal{I}_3$			Avg.
	$\mathcal{S}_a$	$\mathcal{S}_b$	$\mathcal{S}_c$	$\mathcal{S}_a$	$\mathcal{S}_b$	$\mathcal{S}_c$	$\mathcal{S}_a$	$\mathcal{S}_b$	$\mathcal{S}_c$	
container	1.202	1.176	1.186	1.170	1.173	1.154	1.167	1.149	1.168	1.172
<b>grpc</b>	1.002	1.002	1.003	1.003	1.004	1.005	1.002	1.002	1.001	<b>1.003</b>
http	2.337	2.012	1.795	3.719	4.335	1.354	4.985	1.000	1.000	2.504
<b>istio</b>	1.064	1.133	1.090	1.078	1.088	1.084	1.081	1.123	1.086	<b>1.092</b>
node	1.189	1.183	1.182	1.166	1.177	1.164	1.177	1.174	1.177	1.177

By analysing the KPI of each domain attribute one by one manually, we can confirm that the **grpc** and **istio** are strong correlation domain KPIs recording calls of services and GRPC requests, while container, node, and HTTP are the weak correlation that records system resource status, and show the effectiveness of the filter.

TABLE III: Silhouette coefficient of cluster

n_sample	max_radius			
	0.5	1.0	1.5	2.0
250	0.937	0.873	0.805	0.733
500	0.899	0.872	0.785	0.813
750	0.864	0.817	0.783	0.824
1000	0.867	0.813	0.791	0.827

Then, we apply the down-sampling method under the domain to accelerate the cluster, and after calculating the centroid of each cluster, the other KPIs are assigned to the clusters with the smallest DTW from the centroid. Table. III reports the silhouette coefficient result on different sample numbers and  $max\_radius$ , which shows promising results in various settings.

#### D. Effectiveness of Evaluator (RQ3)

Based on the data  $\mathcal{D}$  and  $\mathcal{D}'$  obtained by injecting the original workload and simulated workload, we additionally use the data from two same original workloads  $\mathcal{S}_a$ , namely the zero shape  $\mathcal{S}_o$  for more intuitive evaluation, where the evaluation of  $\mathcal{S}_o$  should be of high similarity. Table. IV reports the result of evaluation between KEWS and WESSBAS by averaging from  $I_1$  to  $I_3$ . Compared to WESSBAS, KEWS achieves better performance on  $\mathcal{S}_o, \mathcal{S}_a, \mathcal{S}_b$ , validating the effectiveness of KEWS. We make other observations as follows. Firstly, the decrease of the KEWS similarity with decreasing shape complexity indicates ESDB is more sensitive to error in smooth curves. Secondly, the small fluctuations in the similarity of WESSBAS reflect its shortcomings in evaluating only static statistics, and its inability to perceive differences at the system level. Thirdly, the overall low value of  $\mathcal{K}_w$  also confirms the effective partition of  $\mathcal{K}_w$  and  $\mathcal{K}_s$ .

TABLE IV: KPIs evaluation result( $\mu_{\mathcal{K}_s} = \mu_{\mathcal{K}_w} = 0.2, \beta = 0.9$ )

Method	Workload Type			
	$\mathcal{S}_o$	$\mathcal{S}_a$	$\mathcal{S}_b$	$\mathcal{S}_c$
WESSBAS	95.3	94.3	94.8	94.5
KEWS( $E_{\mathcal{K}_w}$ )	93.7	95.5	94.5	91.9
KEWS( $E_{\mathcal{K}_s}$ )	99.1	96.3	95.3	93.3
KEWS( $E$ )	98.5	96.1	95.2	93.0

## VI. CONCLUSION

In this paper, we propose ESDB and KEWS to evaluate the similarity between workloads, aiming at the challenges of large-scale, complex characteristics of KPIs in the production environment. Our ESDB measures the similarity of KPIs in terms of shape and intensity and our KEWS, composed of three modules—preprocessing, compression, and evaluation—differentiates between sets of strong and weak correlation KPIs and then evaluates the simulated workload employing ESDB. Extensive experiments demonstrate the superiority of ESDB and KEWS.

## REFERENCES

- [1] B. Hangyu, Y. Kanglin, C. Li, L. Shining, S. Yongjing, Y. Huifeng, T. Ruming, H. Yue, W. Shiqiang, P. Dan *et al.*, “Aioops in practice: Status quo and standardization,” *Journal of Software*, vol. 34, no. 9, pp. 0–0, 2023.
- [2] P. Notaro, J. Cardoso, and M. Gerndt, “A survey of aioops methods for failure management,” *ACM Transactions on Intelligent Systems and Technology (TIST)*, vol. 12, no. 6, pp. 1–45, 2021.
- [3] C. Vögele, A. van Hoorn, E. Schulz, W. Hasselbring, and H. Krcmar, “Wessbas: extraction of probabilistic workload specifications for load testing and performance prediction—a model-driven approach for session-based application systems,” *Software & Systems Modeling*, vol. 17, pp. 443–477, 2018.
- [4] Y. Meng, S. Zhang, Y. Sun, R. Zhang, Z. Hu, Y. Zhang, C. Jia, Z. Wang, and D. Pei, “Localizing failure root causes in a microservice through causality inference,” in *2020 IEEE/ACM 28th International Symposium on Quality of Service (IWQoS)*. IEEE, 2020, pp. 1–10.
- [5] C. Lee, T. Yang, Z. Chen, Y. Su, and M. R. Lyu, “Eadro: An end-to-end troubleshooting framework for microservices on multi-source data,” *arXiv preprint arXiv:2302.05092*, 2023.
- [6] S. Lhermitte, J. Verbesselt, W. W. Verstraeten, and P. Coppin, “A comparison of time series similarity measures for classification and change detection of ecosystem dynamics,” *Remote sensing of environment*, vol. 115, no. 12, pp. 3129–3152, 2011.
- [7] J. Serra and J. L. Arcos, “An empirical evaluation of similarity measures for time series classification,” *Knowledge-Based Systems*, vol. 67, pp. 305–314, 2014.
- [8] J. Paparrizos and L. Gravano, “k-shape: Efficient and accurate clustering of time series,” in *Proceedings of the 2015 ACM SIGMOD international conference on management of data*, 2015, pp. 1855–1870.
- [9] D. J. Berndt and J. Clifford, “Using dynamic time warping to find patterns in time series,” in *Proceedings of the 3rd international conference on knowledge discovery and data mining*, 1994, pp. 359–370.
- [10] J. Lines and A. Bagnall, “Time series classification with ensembles of elastic distance measures,” *Data Mining and Knowledge Discovery*, vol. 29, pp. 565–592, 2015.
- [11] G. Zerveas, S. Jayaraman, D. Patel, A. Bhamidipaty, and C. Eickhoff, “A transformer-based framework for multivariate time series representation learning,” in *Proceedings of the 27th ACM SIGKDD conference on knowledge discovery & data mining*, 2021, pp. 2114–2124.
- [12] Z. Yue, Y. Wang, J. Duan, T. Yang, C. Huang, Y. Tong, and B. Xu, “Ts2vec: Towards universal representation of time series,” in *Proceedings of the AAAI Conference on Artificial Intelligence*, vol. 36, no. 8, 2022, pp. 8980–8987.
- [13] M. Peiris, J. H. Hill, J. Thelin, S. Bykov, G. Kliot, and C. König, “Pad: Performance anomaly detection in multi-server distributed systems,” in *2014 IEEE 7th International Conference on Cloud Computing*. IEEE, 2014, pp. 769–776.
- [14] J. Qian, F. Liu, D. Li, X. Jin, and F. Li, “Large-scale kpi anomaly detection based on ensemble learning and clustering,” *Journal of Cybersecurity*, vol. 2, no. 4, p. 157, 2020.
- [15] M. S. Halawa, R. P. Díaz Redondo, and A. Fernández Vilas, “Unsupervised kpis-based clustering of jobs in hpc data centers,” *Sensors*, vol. 20, no. 15, p. 4111, 2020.
- [16] Z. Li, Y. Zhao, R. Liu, and D. Pei, “Robust and rapid clustering of kpis for large-scale anomaly detection,” in *2018 IEEE/ACM 26th International Symposium on Quality of Service (IWQoS)*. IEEE, 2018, pp. 1–10.
- [17] X. Wang, N. Li, L. Zhang, X. Zhang, and Q. Zhao, “Rapid trend prediction for large-scale cloud database kpis by clustering,” in *2021 IEEE/ACM International Workshop on Cloud Intelligence (CloudIntelligence)*. IEEE, 2021, pp. 1–6.
- [18] G. Yu, Z. Cai, S. Wang, H. Chen, F. Liu, and A. Liu, “Unsupervised online anomaly detection with parameter adaptation for kpi abrupt changes,” *IEEE Transactions on Network and Service Management*, vol. 17, no. 3, pp. 1294–1308, 2019.
- [19] G. Welch, G. Bishop *et al.*, “An introduction to the kalman filter,” 1995.
- [20] A. Basiri, N. Behnam, R. De Rooij, L. Hochstein, L. Kosewski, J. Reynolds, and C. Rosenthal, “Chaos engineering,” *IEEE Software*, vol. 33, no. 3, pp. 35–41, 2016.
- [21] D. F. Silva and G. E. Batista, “Speeding up all-pairwise dynamic time warping matrix calculation,” in *Proceedings of the 2016 SIAM International Conference on Data Mining*. SIAM, 2016, pp. 837–845.
- [22] H. Sakoe and S. Chiba, “Dynamic programming algorithm optimization for spoken word recognition,” *IEEE transactions on acoustics, speech, and signal processing*, vol. 26, no. 1, pp. 43–49, 1978.
- [23] Y. Han, Q. Du, J. Xu, S. Zhao, Z. Chen, L. Cao, K. Yin, and D. Pei, “Lws: A framework for log-based workload simulation in session-based sut,” *Journal of Systems and Software*, vol. 203, p. 111735, 2023.
- [24] C. Wang, K. Wu, T. Zhou, G. Yu, and Z. Cai, “Tsagen: synthetic time series generation for kpi anomaly detection,” *IEEE Transactions on Network and Service Management*, vol. 19, no. 1, pp. 130–145, 2021.